Int. J. Electrochem. Sci., 10 **(2015)** 3301 - 3318

International Journal of ELECTROCHEMICAL SCIENCE
www.electrochemsci.org

Review

Recent Progress in Electrode Fabrication Materials and Various Insights in Solar cells: Review

Rasu Ramachandran[2], *Veerappan Mani*[1], *Shen-Ming Chen*[1,*], *George peter Gnana kumar*[3], *Pandi Gajendran*[2], *Natarajan Biruntha Devi*[4], *Rajkumar Devasenathipathy*[1]

[1]Electroanalysis and Bioelectrochemistry Lab, Department of Chemical Engineering and Biotechnology, National Taipei University of Technology, No.1, Section 3, Chung-Hsiao East Road, Taipei 106.Taiwan (ROC).
[2]The Madura College, Department of Chemistry, Vidya Nagar, Madurai – 625 011, Tamil Nadu, India.
[3]Department of Physical Chemistry, School of Chemistry, Madurai Kamaraj University, Madurai-625 021,Tamil Nadu, India.
[4]Department of Chemsitry, S. Vellaichamy Nadar College, Nagamalai, Madurai – 625019, Tamil Nadu, India.
[*]E-mail: smchen1957@gmail.com

Received: 13 December 2014 / *Accepted:* 25 December 2014 / *Published:* 24 February 2015

In recent times, substantial progress have been made in the development of primary and applied aspects of solar cells especially in light weight materials and low-cost electrode materials for the improvement of power generation devices. Various new strategies, methods and innovative approaches were implemented in organic, bulk-heterojunction, polymer and dye-sensitized solar cell applications to increase the overall power conversion efficiencies. Herein, we review the recent developments made in electrode materials based on carbon, metal oxides, polymers and nanocomposites for the development of solar cells. In addition, progresses made in the fabrication methods (coating and printing methods) have also been reviewed. The important factors such as solvents, temperature and atmosphere are also discussed. Special attention has been given to the characterization methods reported for the DSSCs.

Keywords: Solar cells, electrode materials, organic solar cells, bulk-heterojunction solar cells, dye-sensitized solar cell, energy devices.

1. INTRODUCTION

Solar cells are promising green energy resources which convert abundant light energy into electrical energy [1]. Recently, there have been extensive developments in dye-sensitized solar cells

(DSSCs) which can be controlled by high surface area of photoanode to enhance power conversion efficiency values [2]. There are few reviews which are addressed the fabrication and different techniques for the preparation of electrode materials and application of solar cells [3-9]. During last two decades, conducting polymers (polyaniline (PANI), polyhexylthiophene, poly(3,4-ethylenedioxythiophene) (PEDOT) and polypyrrole (Ppy)) have established considerable attention for the fabrication and developments of solar cells applications [10-13]. Sol-gel becomes a popular method to produce molecular level homogeneity, colloidal suspension and large-scale quantity for DSSCs applications [14-16]. New kinds of innovative materials have been expanded at a rapid pace since the discovery of DSSC in 1991 by Michael Gratzel and his co-workers [17].

DSSCs are promising next generation solar energy conversion system due to their potential low-cost electrode materials; however, their performances are mainly depends on the choice of electrode materials, solvents and annealing conditions etc. [18]. Ramasamy and his co-workers [19] reported, a ferrocene-derivate mesocellular carbon foam (Fe-MCF-C) counter electrodes for DSSCs which can yield power conversion efficiencies upto 7.89 %. Interestingly, Reel-to-reel (R_2R) solvent based solar cells have been fabricated by slot-die wet coating method and the fabricated electrodes yielded efficiency value of 3.2 % [20]. Poly(3,4-ethylenedioxythiophene) (PEDOT)/fluorinated tin oxide (FTO) composite film modified electrode deliberate as a promising alternative electrode materials for platinum free DSSCs. The electrode showed faster reaction rate and higher electrocatalytic activity for I^{3-} reduction which is due to increased open circuit potential and short-circuit potential (V_{OC}) [21]. Theuring *et al* [22] studied oxide-metal oxide (aluminium zinc oxide-Ag-aluminium zinc oxide) electrode which exhibited highly improved efficiency of 30 %. Low-defect and water soluble microwave exfoliated graphene nanosheet/platinum nanoparticle composite has been prepared by oxidative intercalation, microwave exfoliation and ultrasonication methods and used in DSSCs [23]. The enhancement and low temperature optimized conditions of conducting polymer (PEDOT:PSS) composite were prepared by *in-situ* method for DSSCs studies [24].

A systematic analysis of thieno[3,4-b]thiophene/benzodithiophene (PTB7) (6,6)-phenyl-C_{71} butyric acid methyl ester ($PC_{71}BM$) composite has been investigated in various solvents including methanol, ethanol, DMSO, acetone and isopropanol [25]. From this comparative study, methanol exhibits high Δ value and low viscosity and significantly increased the overall efficiency from 6.55 to 8.13 %. Fig.1 (a, b) presents the device architecture and schematic energy of flat band for the polymer solar cells (PSC) analysis. A n-type Si:H/C-Si hetero-junction solar cell has been synthesized using mono-like silicon wafer which able to reach the energy conversion efficiency upto 21.5 % [26]. On the other hand, Mishima *et al* [27] developed a highly efficient hetero-junction with intrinsic thin-layered (HIT) solar cell which exhibited V_{OC} of 743 mV and efficiency of 22.8 %.

This review article explores the new developments of electrode fabrication methods and different kinds of electrode materials reported in organic, bulk-heterojunction, polymer and DSSC applications. The article paper mainly focused on low-cost electrode materials, fabrication of different kind of composites, highest power conversion efficiency value and long durability.

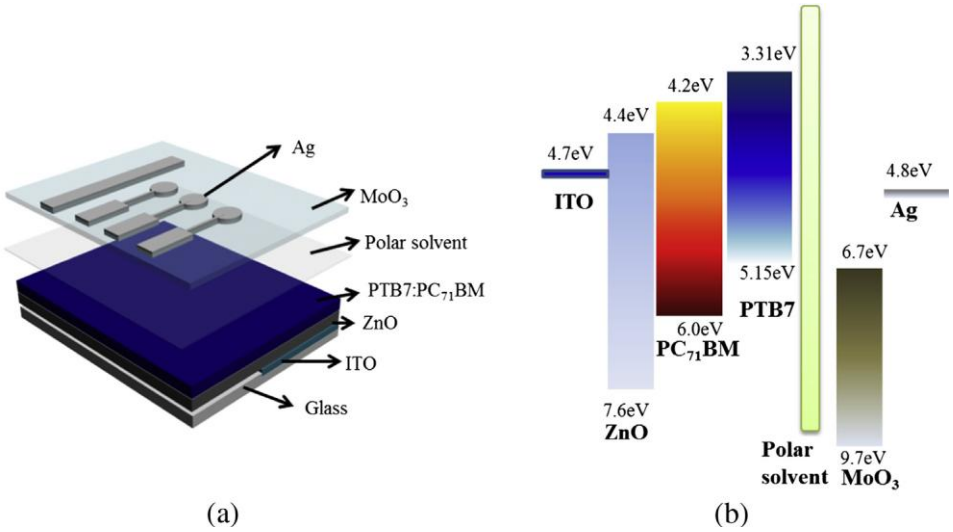

Figure 1. Device architecture of PSCs (a) and schematic energy diagrams for flat band conditions of PSCs (b). (Reproduced with permission from ref. [25]).

2. ELECTRODE MATERIALS FOR SOLAR CELLS DEVELOPMENT

Several new versatile nanostructured electrode materials have been reported for the development of solar cell applications, such as carbon electrodes (Single-walled carbon nanotube (SWCNT), multi-walled carbon nanotube (MWCNT), graphene oxide (GO) and fullerene), metal oxides (TiO_2, fluorinated tin oxide, SnO_2, boron doped ZnO and Cu_2O) and conducting polymers (Poly(3,4-ethylenedioxythiophene), poly(styrenesulfonate) (PSS), poly-3-hexylthiophene and polyaniline) electrodes etc. These types of electrode materials were greatly enhanced the power conversion efficiency (η) of the solar cells.

2.1. Carbon electrodes

Among carbon electrodes, carbon nanotubes (SWCNT and MWCNT) which were discovered by Iijima [28] in 1991 are the most promising electrodes for the solar cell applications. Carbon nanotubes (CNT) possess unique mechanical and electronic properties. Moreover, graphene and MWCNT nanocomposite has been prepared and used as counter electrode in DSSCs [29]. Zhu *et al* [30] overviewed various carbon based electrode materials used in photovoltaic cells (PVC), such as organic solar cells, silicon based solar cells and DSSC. SWNT-polyvinyl pyrrolidone (PVP) composite was prepared by simple casting technique and the composite incorporated solar cell exhibited power conversion efficiency of 4.5 % with high V_{OC} (718 mV) and J_{SC} (12.14 mA cm^{-2}) [31]. A hard carbon spherule (HSC) was used as a counter electrode for DSSCs which can render 5.7% of conversion efficiency [32]. A fullerene derived poly(3-hexylthiophene:phenyl-C_{61}-butyric acid methyl ester (P3HT:PCBM) films were synthesized by ink-jet printing method and employed for high performance solar cell applications [33]. Susarova *et al* [34] reported a systematic analysis of seven different bis-

cyclopropane adduct solvents to enhance the performance of the organic bulk-heterojunction solar cells.

2.2. Metal oxide electrodes

Metal oxide electrode materials emerged as another important class of functional groups covering solar cell applications [35]. Thin layer of titanium oxide [36] and zinc oxide films [37] have been synthesized by using sol-gel method and used for solar cell applications. These electrodes absorbed UV light, but transparent in the visible region. Electrochemically deposited nanoporous ZnO on FTO electrode do not favor in the photoelectrode studies and limited PCE value of about 2.4 % was obtained [38]. The studies proved that TiO_2 based electrodes presenting better performances than the ZnO based nanofibres. Kang *et al* [39] fabricated a near infra-red transparent film electrode by multi-cathode magnetron sputtering method with GeO_2 and In_2O_3 as target. The resulting bulk-heterojunction of organic solar cell exhibited good cell performance with a fill factor (FF) of 67.38 %, J_{SC} of 8.438 mA cm^{-2} and PCE of 3.44 %. Aluminium doped zinc oxide (AZO) nanoparticles were prepared in isopropyl alcoholic medium and used with different stablizers (Polyvinylpyrrolidone, acetyl acetone and 3,6,9-trioxydeconoic acid) which exhibited higher efficiency in inverted solar cell applications [40]. A cobalt-doped nickel oxide and activated carbon electrodes have been used for DSSC which as produced 4.9 % of energy conversion efficiency [41].

2.3. Polymer electrodes

PSCs attracted significant attention owing to their potential advantages such as large surface area and low-cost [42, 43]. PSCs are mainly used to improve the electrode sensitivity, selectivity, broad absorption properties, charge carrier mobility and high stability. A semi-transparent and surface free polymer (PEDOT:PSS) electrode has been fabricated by spray coating method and evaluated in organic solar cells studies, the evaluated semi-transparent electrodes power conversion efficiency (η) of 2 % [44]. Roesch *et al* [45] reported a non-inverted polymer (Poly[9-(1-octylnonyl)-9H-carbazol-2,7-diyl]-2,5-thiophenediyl-2,1,3-benzothiazol-4,7-diyl-2,5-thiophenediyl (PCDTBT)):Phenyl C_{61} butyric acid methyl ester composite based solar cells sealed with TiO_2/Al which leads to a notable improvement in the efficiency with durability of 18,000 hrs under ambient conditions. The cathode inter layer of zwitter ionic ammonium molecule and neutral amino organic molecules are introduced into inverted polymer (Poly[4,8-bis(2-ethylhexyloxyl) benz[1,2-b:4,5-b'] dithiophene-2,6-diyl-alt-ethylhexyl-3-uoro thithieno [3,4-b] thiophene-2-carboxylate-4,6-diyl] (PTB7)):(6,6-phenyl-C_{71}-butyric acid methyl ester ($PC_{71}BM$) blend and it was used as a photo active electrode which exhibited highest power conversion efficiency of 8.07 % [46]. Bulk hetero junction PCDTBT:$PC_{71}BM$ solar cells have been fabricated with polyaniline:camphor sulfonic acid/polyethylene terepthalate (PANI:CSA/PET) and PANI:CSA/polyethylene napthalate (PANI:CSA/PEN) composite electrodes which are exhibited outstanding performance in terms of energy conversion efficiencies [47].

2.4. Nanocomposite electrodes

Recently, nanocomposites are inevitable electrode materials in all kinds of electrochemical applications including sensors [48], biosensors [49, 50], supercapacitors [51], batteries and solar cells etc. The combination of two or more dissimilar materials can be used to control the morphological behaviour and for the improvement of overall activities. Wang *et al* [52] reported MWCNT/polypyrrole composite as an efficient counter electrode for DSSC and obtained PCE of 6.2 %. Low-defect and water soluble graphene nanosheet/platinum nanoparticles composite has been prepared for DSSC which able to obtain the efficiency of 6.69 % [53]. A inverted organic solar cells based on reduced graphene oxide (RGO)/Titanium oxide (TiO_x) composite has been successfully prepared by sol-gel method [54], the resulting solar cells produces short circuit current of 9.85 mA cm^{-2} and PCE of 3.82 %. Stubhan *et al* [55] reported highest performance value of fill factor and PCE value were markedly enhanced by using silver nanowire/metal oxide (AgNWs) composite ie FF of 62 % and PCE of 2.7 %. Stubhan *et al* [55] reported high performance solar cell based on silver nanowire/metal oxide composite with greatly enhanced FF of 62 % and PCE of 2.7 %.

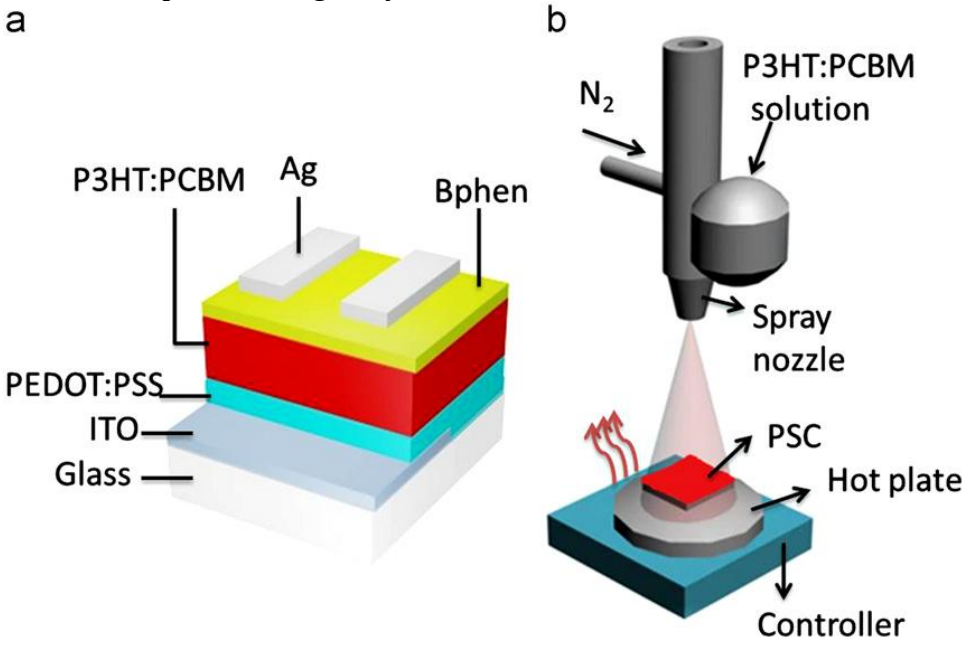

Figure 2. Schematic of (a) spray coated PSC and (b) spray coating apparatus. (Reproduced with permission from ref. [56]).

3. SOLAR CELLS FABRICATION TECHNIQUES

3.1 Coating method

A polymer solar cell based on ITO/PEDOT:PSS:P3HT:PCBM:Bpheng/Ag composite has been fabricated using spray coating technique at various annealing temperatures (fig.2) [56]. Xiong *et al* [57] used two different (Doctor Blading and spin coating) techniques for the fabrication of a novel polymer blended SCs. The authors found that homogeneous and uniform film was obtained from

doctor blading method compared with spin coating of PSCs applications. As a result, Doctor Blading method exhibited higher PCE (4.46 %) compared with spin coated method. TiO_2 nanoparticles film has been fabricated on stainless steel mesh by three different techniques (Sol-gel, dip coating and sputter coating method) and their DSSC performance have been studied [58]. Mohammed *et al* [59] reported the preparation of copper indium di-selenide (CIS) thin film by electro spray deposition technique (ESD) under room-temperature atmospheric condition for the solar cell applications. Polypyrrole/functionalized MWCNT films on rigid FTO and flexible ITO coated polyethylene napthalate substrates have been prepared which are exhibited good PCE performance of 7.02 % and 4.04 % under room-temperature respectively [60].

3.2 Printing methods

A flexible transparent copper nano wire mesh has been fabricated by simple transfer printing from flexible poly(dimethyl siloxane) as potential replacement for ITO electrodes in OSCs [61]. These electrodes have great potential to replace ITO for the making of low cost and large area flexible of OSCs. Kopola *et al* [62] used polymer (poly-3-hexyl thiophene (P3HT) and [6,6]-phenyl-C61-butyric acid methyl ester (PCBM) blend) based solar cells fabricated by high-throughput roll-to-roll (R_2R) gravure printing method. The important parameters such as printing speed, ink properties and printability of the photoactive as well as the hole transport layer studies are optimized. In gravure printing method studies, the important printing parameters like ink viscosity, surface roughness, surfactance, surface energy and surface modification by plasma cleaning have been optimized to achieve homogeneous printing of multi layer organic photovoltaic (OPV) devices [63]. The authors tested highly boiling solvents (chlorobenzene, ortho-1,2-dichlorobenzene, 1,2,4-trichlorobenzene and 1,2,3,4-tetrahydro naphthalene) for P3HT:PCBM which showed Arrhenius behaviour up to 8 wt %. Airbrush spray-coating is one of the fabrication methods developed for the preparation of polymer heterojunction solar cell device which reported the power conversion efficiency of 4.1 % with good reproducibility [64]. Fig.3. shows a schematic illustration of three different printing methods for developing an inverted organic solar cell [65]. Kopola *et al* [66] used a new kind of aerosol jet printing method for the fabrication of ITO free organic solar cells with an inverted layer sequence. The controlled printing parameters have been optimized such as chuck temperature, printing speed and number of printing passes.

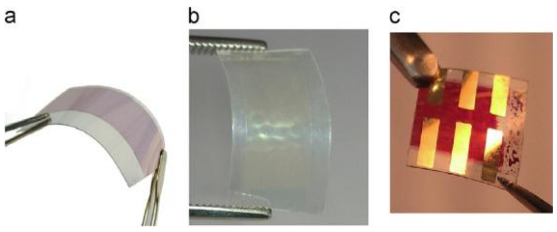

Figure 3. (a) printed 15% P3HT:PCBM 1:1 in *o*DCB on PET/ITO (b) TiO*x* dissolved in IPA, printed on PET/ITO, 100 lines cm^{-1} 0 shape and (c) an inverted organic solar cell with, spin coated TiO*x*, PEDOT:PSS þ20 % IPA, a device with a printed P3HT:PCBM (15 % in *o*DCB). (Reproduced with permission from ref. [65]).

4. INFLUENCE FACTORS IN DSSC

4.1. Effect of solvents

A systematic study of DSSCs can be used at different solvent medium; this is associated with the structural and electronic distribution changes. Low volatile solvents are friendly atmospheric nature and they give different physical and chemical properties to the dye adsorbed on the counter electrode surface [67]. In one interesting report, a simple organic dye of CD-7 was dissolved in different solvents like DMF and THF to sensitize TiO_2 photoelectrode [68, while From CD-7 dye sensitized TiO_2 film on THF bath exhibited larger adsorption energy value than that of DMF bath. Zhang *et al* [69] used a systematic analysis of the effects of different polar solvent on the photovoltaic performance of thieno [3,4-b] thiophene/benzodithiophene (PTB7):(6,6)-phenyl-C_{71} butyric acid methyl ester ($PC_{71}BM$). Methanol medium exhibited higher Δ value and low viscosity which could present a remarkable enhancement in the power conversion efficiency value from 6.55 % to 8.13 %. Chen *et al* [70] reported IPCE and curve-voltage curve (fig. 4) of DSSCs at two different solvent medium such as THF and DMF. The THF-CD-7-TiO_2 based DSSC exhibited η value of 1.53 % which is two times higher than that of DMF-CD-7-TiO_2 based DSSC.

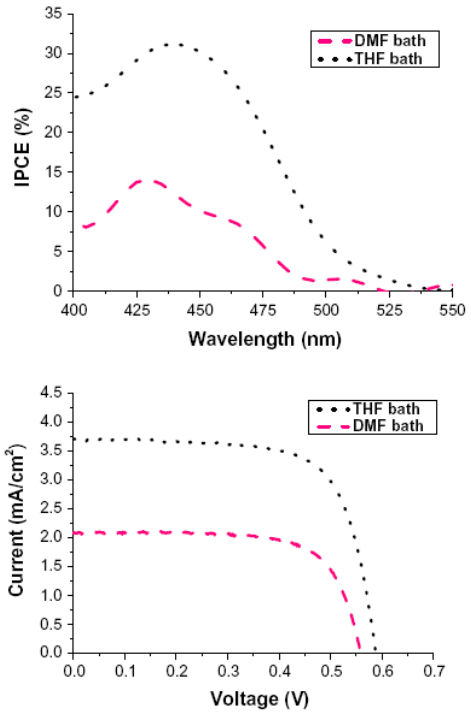

Figure 4. IPCE spectra and *J–V* curves of DSSCs based on CD-7 sensitized by different solvents. (Reproduced with permission from ref. [70]).

4.2. Effect of temperature

In DSSCs, temperature is one of the essential parameter which affects the contact angle values; as the contact angle value decreases, the temperature increases [71]. Large area compatible p-type

nanocrystalline silicon has been synthesized by DC sputter coat method which has the possibility of enhancing the DSSC performance at room temperature [72]. Sing and Ravindra [73] theoretically overviewed the temperature dependence of solar cell studies in the range from 273-523 K. The value of V_{OC} is decreases, while the value of J_{SC} increases upon increasing temperature. The fig. 5 shows the current-voltage and power-voltage studies of the silicone solar cell investigated under illumination intensity of 1000 W m^{-2} at different optimized temperatures [74]. These results revealing that as temperature increases, the value of J_{SC} also increases simultaneously, while the value of V_{OC} decreases.

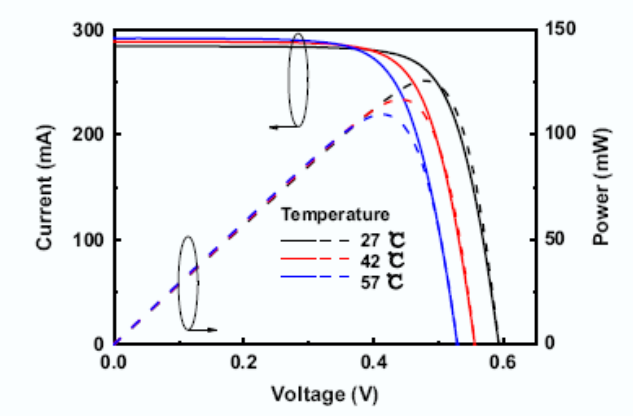

Figure 5. Current–voltage (*I–V*) and power–voltage (*P–V*) characteristics of solar cells under their radiance intensity of 1000W m^{-2} at different temperatures. (Reproduced with permission from ref. [74]).

4.3. Effect of atmosphere

Guechi *et al* [75] studied the effects of variation of water vapour performance by using two different solar cells such as nano crystalline silicon (nc-Si:H) and cadmium telluride (CdTe) which are exhibited efficiency value of 2.38 % and 3.15 % respectively. These results clearly indicated that the efficiency value for both the cells increases with increasing water vapour. The solar power plants are often affected by the influence of acid rain atmosphere of SO_2 on the durability [76]. After exposure of the acid rain atmosphere, the deterioration and reflectance drop was smaller in the thick glass mirror than thin glasses. In one report, Nb-TiO_2 electrode doped with conducting organic polymer of MEH-PPV showed higher hybrid solar cells (HSC) performance than bare TiO_2 based HSC [77]. Here, TiO_2/MEH-PPV composite has been prepared under atmospheric conditions. Nan *et al* [78] used CdS nanorod arrays (NRs)/poly[2-methoxy-5-(2'-ethylhexyloxy)-1,4-phenylene vinylene] (MEH-PPV) composite for HSC which is stable under ambient atmospheric conditions. Gimpel *et al* [79] studied the silicon wafer atmospheric study of aluminium back surface field (Al-BSF) solar cells by using an infra-red active secondary laser sulphur n-doped emitters an attractive path for the enhancement of PCE. In addition, a polymer solar cells made of PTB7:PCBM has been investigated at two different environmental conditions (Inert and atmosphere) and the results revealing that atmosphere plays a crucial in the overall efficiency [80]. Fig. 6. presents the optimized *J–V* curve under inert condition

which seems favorable than atmospheric conditions due to the photo-oxidation and low-band gap polymers.

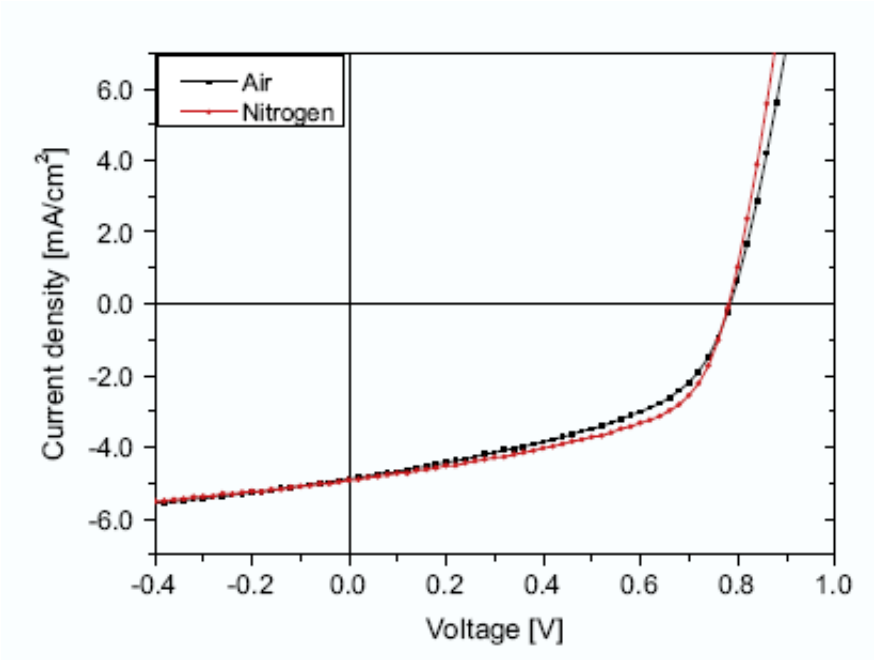

Figure 6. *J–V* curve dependence on preparation atmosphere. (Reproduced with permission from ref. [80]).

5. CHARACTERIZATION STUDY IN DSSC

5.1. Cyclic voltammetry

Hong *et al* [81] discussed the voltammetric behaviour of three different electrode materials such as Pt, PEDOT-PSS (poly(3,4-dioxy thiophene)-poly styrene sulfonate) and graphene/PEDOT-PSS composite. Fig. 7 shows the voltammogram obtained as two pairs of redox behaviour such as I^2/I^{3-} (positive pair) and I^{3-}/I^- (negative pairs). Similarly, polyaniline electrode was used as a counter electrode and the catalytic activity towards I^-/I^{3-} redox couple was investigated. The two pairs of redox reaction were observed like the reduction of I^-/I^{3-} and oxidation of I^2/I^{3-}. In this reaction, the catalytic activity of PANI electrode exhibited higher peak current density than Pt electrode [82]. Uppachai *et al* [83] used the low cost tungsten oxide (WO_{3-x}) as a counter electrode in which annealed temperature range between 500-600ºC able to produce greatly enhanced power conversion efficiency.

Three different triphenylamines sensitizers such as $TPACR_1$, $TPACR_2$ and $TPACR_3$ with different molecular orbital energy level have been coated on TiO_2 [84]. The LUMO and HOMO level of the three ($TPACR_1$, $TPACR_2$ and $TPACR_3$) dyes are suitable for the conduction band of TiO_2 electrode and redox potential of the iodine/iodide.

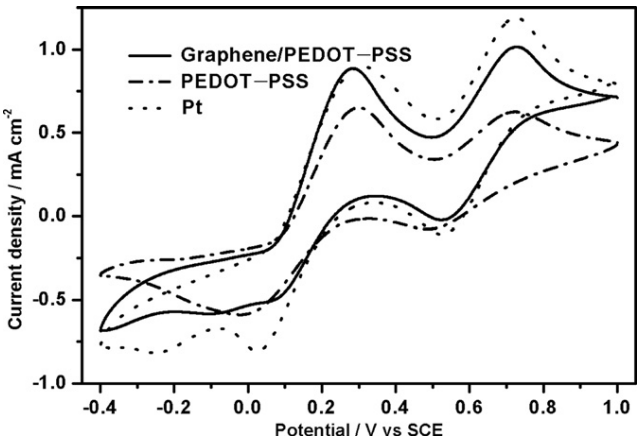

Figure 7. Cyclic voltammograms for graphene/PEDOT–PSS composite with 1 wt % graphene, PEDOT–PSS and Pt electrode in acetonitrile solution of 10 mmol L^{-1} LiI, 1 mmol $L^{-1}I_2$, and 0.1 mol L^{-1} $LiClO_4$ at a potential scan rate of 20 mV s^{-1}. (Reproduced with permission from ref. [81]).

5.2. Raman studies

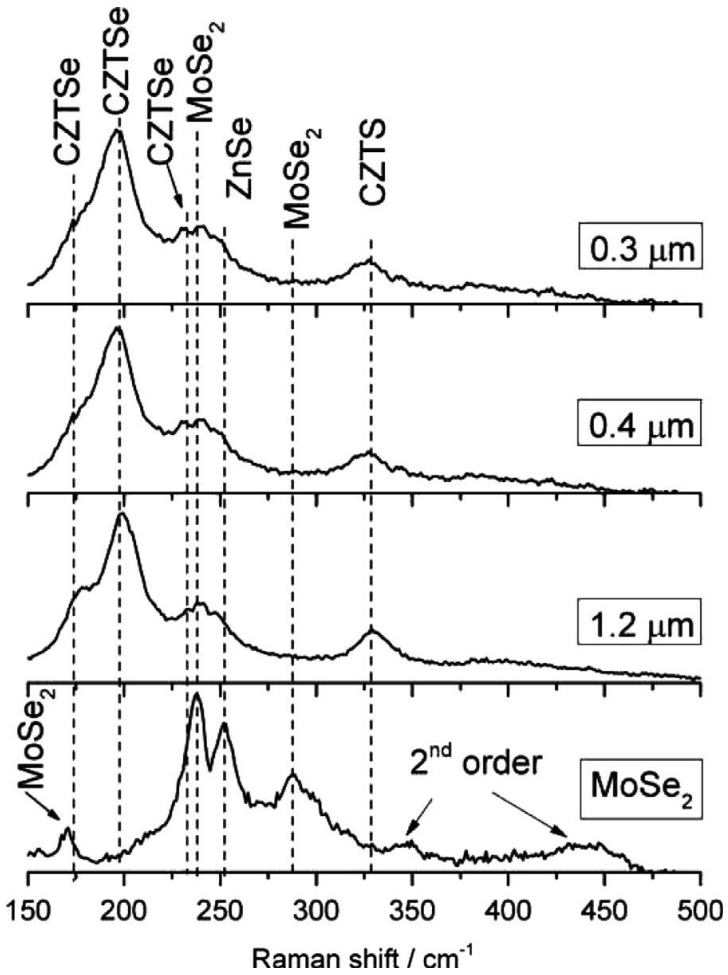

Figure 8. Raman spectra of the selenized samples measured after scratching the sample in order to remove material to the different depths as listed. (Reproduced with permission from ref. [90]).

Nickel oxide/graphene composite has been synthesized by chemical exfoliation method [85]; where the composite was examined by using Raman spectroscopy which showed D band at 1349 cm^{-1} and G band at 1587 cm^{-1}. The composite (NiO/graphene) clearly indicates a strong interaction between NiO and graphene sheets. Yin *et al* [86] used a monocrystalline ZnO nanorods (NRs) on RGO by electrochemical method; Raman study of RGO/ZnO NRs exhibited two identical peaks occur at 1350 and 1590 cm^{-1}, this could assign to D and G band of RGO. Similarly, Raman spectra has been used to characterize the solar cell materials in these reports [87-89]. Romanyuk *et al* [90] reviewed a specific group of non-vacuum method for the preparation of kesterite solar cell. Raman spectrum (fig.8) of selenized samples were measured at different depth materials conditions. For these depths of 0.3 mm, 0.4 mm and 1.2 mm, the corresponding reported kesterite phase (I^{st} A_1 mode at 329 cm^{-1}, II^{nd} A_1 mode at 196 cm^{-1} and III^{rd} additional mode 233 cm^{-1}) have been identified.

5.3. Impedance studies

Nyquist plots have also widely used to study the solar cells. For instance, two different perovakite solar cell film materials such as spin coat titanium oxide (SC-TiO_2) and thermal oxidation method titanium oxide (TO-TiO_2) [91] have been prepared and studied.

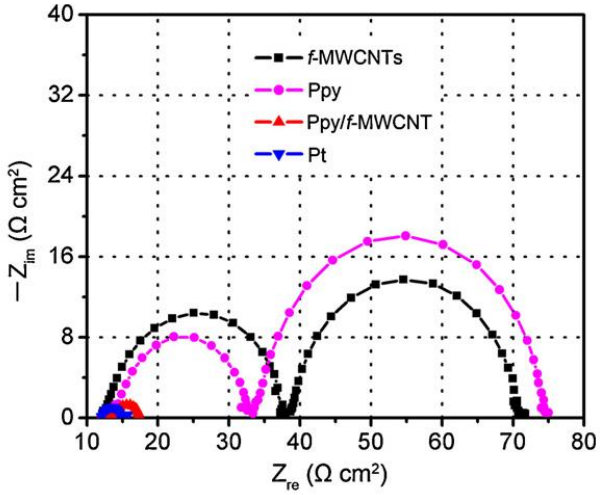

Figure 9. Nyquist plots for the counter electrodes (f-MWCNTs, Ppy, Ppy/f-MWCNT, and Pt), respectively (a) and the magnified view for the Ppy/f-MWCNT and Pt counter electrode. (Reproduced with permission from ref. [60]).

From the EIS analysis, the perovskite solar cells with the TO-TiO_2 compact film have a lower R_s value than that with the SC-TiO_2 compact film. Kavan *et al* [92] have prepared five different graphene nano plates coated on optically transparent thin film (FTO). The two different (FTO/TiO_2/3 and FTO/TiO_2/4) dye interface electrodes were performed with EIS studies for a useful tool to estimate the electron recombination resistance efficiency value [93]. The value of R_{CT} under dark conditions for FTO/TiO_2/3 and FTO/TiO_2/4 composite were of 10.4 and 43.3 Ω cm^2. This is clearly indicated, the decreased R_{CT} value for FTO/TiO_2/3 electrode than FTO/TiO_2/4 by light conditions. Kim *et al* [94]

used the polymer hybride quantum-dot-sensitized solar cell for the development of using CdSe/CdS/ZnO composite as a photo anode and P3HT as a conjugate polymer. Fig.9. showed the EIS analyses of four different (Pt, Ppy, f-MWCNT and Ppy/f-MWCNT) samples were deposited on FTO glass substrate [60]. From the EIS analysis, the obtained R_{CT} value (1.81 Ω cm^2) of Ppy/f-MWCNT composite lower than that of other electrodes which was clearly indicated that high electrical conductivity and better electrocatalytic activity.

5.4. Solar energy conversion efficiency

Energy conversion efficiency is one of the important parameters in DSSCs. Lee *et al* [95] used two (short-ZnO and long arm-ZnO) different tetrapod-like ZnO nanostructured materials which were synthesized by DC plasma technique. The DSSCs of S-ZnO exhibited higher PCE value than that of L-ZnO. This result could explain by the fact that the thickness of photo electrode for N719 sensitized tetrapod ZnO cell was optimized at 26 µm (S-ZnO). Similarly, the optimized photo electrode cell thickness value of 36 µm was estimated for L-ZnO. The reported power enhancement conversion efficiency values of DSSCs were 4.78 % and 4.07 % for S-ZnO and L-ZnO respectively. A high performance electrode material of GaAs with dual layer of CdS quantum dots (QDs) was studied by poly dimethoxy siloxane (PDMS) [96]. A two different $CuInGaSe_2$ (CIGS) based solar cells such as CIGS/t-CdS/ZnO:B and CIGS/vt-CdS/Zn(O,S)/ZnO:B have been reported [97]. By using these electrode materials, the energy conversion efficiency values of 16.2 % and 66.5 % have been obtained. A high performance metal wrap (HIP-MWT) solar cell was reported, where the stimulated efficiency and half gap width measurements are obtained (fig.10) [98]. Our research group reported DSSCs based on ZnO/MWCNT nanocomposite [99], platinum-ruthenium bimetallic nanoparticles/PEDOT [100], iodine-PEDOT composite [101], Pumpkin stem-derived activated carbons [102], graphene-TiO_2 composite [103] and poly(Brilliant Cresyl Blue)/MWCNT [104] with appreciable power conversion efficiencies.

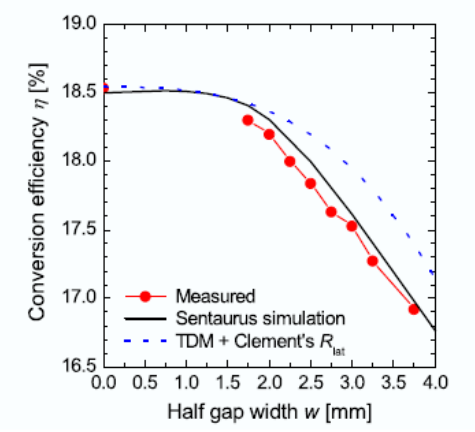

Figure 10. The simulated efficiency as a function of half gap width decreases for both cells in accordance to the measurement. The measured linear decrease is better reproduced with the 2D Sentaurus simulation compared to the analytical approach using the two-diode model (TDM) and Clement's expression for the lateral series resistance (Reproduced with permission from ref. [98]).

5.5. Incident photon to current efficiency (IPCE)

IPCE can be used to measure the spectral response of the cell and quantum efficiency of photo current generation. Radio frequency (RF) and direct current (DC) sputtering are viable methods to form ZnO/Ag/MoO_3 (ZAM) multi-layer electrode used for bulk-heterojunction OSCs [105]. The optimized transparent composite electrode (TCE) exhibited maximum IPCE value of 60 % and 38 % at the wavelength of 540 nm and 500 nm respectively (fig.11). A diode (Au/TiO_2 10 nm thickness) of metal oxide composite film has been used to measurement of incident photon to current efficiency [106]. Accordingly at a film electrode, the steady state photoelectric current is given by (Eq.1)

$$I = \frac{c(h\nu - \varphi)^n}{h\nu} \quad (1)$$

Where *c*- is constant, by applying Flower's law, the fitting parameter *n*-value is 2 and φ is the Schottky barrier height [107]. Morandeira *et al* [108] recently reported a peryleneimide sensitizer covalently linked with peryleneimide dyad for DSSC applications, which has three fold enhancements in live charge separation and absorption. The low IPCE value occured at large incident light intensity was due to the diffusion limitation of the electrolyte [109]. Table 1 shows the DSSC performance of platinum free electrodes which are exhibited excellent performances compared with platinum based DSSCs.

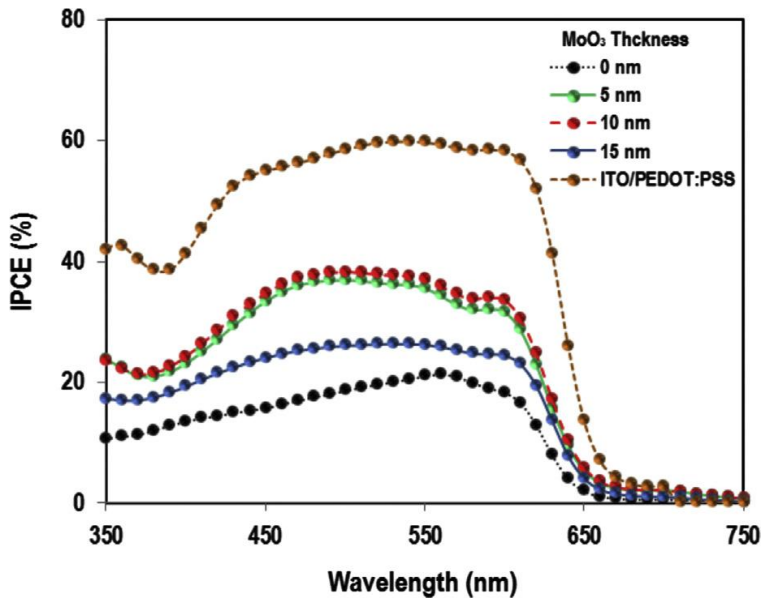

Figure 11. IPCE for ZAMTCEOSCs as a function of MoO_3 thickness and OSC fabricated on a ITO substrate with PEDOT: PSS as a hole transport layer. (Reproduced with permission from ref. [105]).

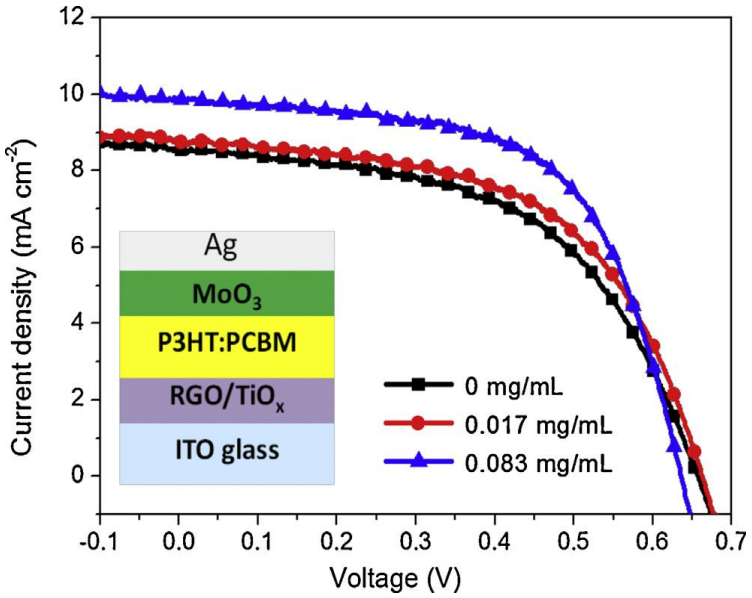

Figure 12. *J-V* characteristics of the inverted P3HT:PCBM solar cells incorporating with MoO_3 hole transport layer and RGO/TiO_x electron transport layer. The inset shows the device structure of inverted cell. (Reproduced with permission from ref. [54]).

Table 1. Comparison of DSSC performances of alternative electrode materials (Pt free) reported for DSSCs.

S.No	Electrodes	J_{SC} (mA cm^{-2})	V_{OC} (mV)	FF (%)	Efficiency (%)	References
1	ZnO replica	15.6	879	74	10.1	[114]
2	FTO/PANI	15.24	710	0.604	6.54	[115]
3	2D Graphene	16.29	690	62	6.97	[116]
4	TiN-CNTs	12.74	750	0.57	5.41	[117]
5	Heteroleptic polypyridyl Ru complex C_{101}	5.42	746	0.833	11.3	[118]

V_{OC} = Open circuit potential, J_{SC} = Short-circuit current density, FF = Fill factor, η = Energy conversion efficiency

5.6. Current-voltage (I-V) study

A nitrogen-doped 3D graphene foam electrode has been reported as a metal-free electrocatalyst for the reduction of tri iodide reaction [110]. The N-doped graphene electrode demonstrated that the current-voltage study exhibited current density (J_{SC}) value of 15.84 mA cm^{-2} and power conversion efficiency value of 7.07 %. N-doped graphene electrode can be used as a low cost alternative counter electrode material than platinum based electrodes [111]. The DSSCs value of graphene nanosheet electrode exhibited 6.81 % efficiency, which is near to the efficiency obtained with platinum electrode. Guo *et al* [112] used a rectangular bunched TiO_2 nanorod (NR) array on carbon fibers (CFs) for DSSCs. The TiO_2 NRs-coated CFs used as a photo anode able to give efficiency of 1.28 % with J_{SC}

value of 4.58 mA cm^{-2}. In another report, polyvinylpyrrolidone (PVP)-modified Al-doped ZnO electrode exhibited J_{SC} of 11.30 mA cm^{-2} and PCE of 2.86 % [113]. Similarly, PVP-Al modified electrode exhibited J_{SC} of 11.57 mA cm^{-2} and PCE of 4.08 %. The inverted organic solar cell of RGO/TiO*x* composite has been synthesized by sol-gel method [54]. The *J-V* characterization (fig.12) of inverted P3HT:PCBM:RGO/TiO*x* exhibited J_{SC} of 9.85 mA, PCE of 3.82 % and FF of 61 %.

6. CONCLUSIONS

In summary, during the last two decades, carbon based electrode (SWCNT, MWCNT, graphene oxide, fullerene and carbon nano fibre), metal oxides (TiO_2, Aluminium doped ZnO, fluorinated tin oxide, GeO_2 and In_2O_3) and conducting polymers (polyaniline, polyhexylthiophene, poly(3,4-ethylenedioxythiophene) and polypyrrole) are proved as promising electrode materials the fabrication of all types of solar cells. However, the efficiency of the solar cells varies with different electrodes and based on types of the solar cell. The future work should be focused more in finding appropriate ways to prepare cost effective solar cells with high performance photovoltaic applications.

ACKNOWLEDGEMENT
This research work was supported by Ministry of Science and Technology, Taiwan and India-Taiwan Science and Technology Cooperation program, DST, India.

References

1. B.A. Gregg, A. Zaban, S. Ferrere, *Phys. Chem. Chem. Phys.*, 212 (1999) 11.
2. J.W. Ondesma, T.W. Hamann, *Coord. Chem. Rev.*, 257 (2013) 1533.
3. H. Cao, W. He, Y. Mao, X. Lin, K. Ishikawa, J.H. Dickerson, W.P. Hess, *J. power sources* 264 (2014) 168-183.
4. H. Wang, Z. Guo, S. Wang, W. Liu, *Thin Solid Films,* 558 (2014) 1.
5. A. Terakawa, *Sol. Energy Mater. Sol. Cells,* 119 (2013) 204.
6. J. You, L. Dou, Z. Hong, G. Li, Y. Yang, *Prog. Polym. Sci.*, 38 (2013) 1909.
7. C.M. Proctor, M. Kuik, T.Q. Nguyen, *Prog. Polym. Sci.*, 38 (2013) 1941.
8. F.C. Krebs, Solar energy materials & solar cells 93 (2009) 394.
9. G.M.M.W. Bissels, J.J. Schermer, M.A.H. Asselbergs, E.J. Haverkamp, P. Mulder, G.J. Bauhuis, *Sol. Energy Mater. Sol. Cells*, 130 (2014) 605.
10. Y. Saito, W. Kubo, T. Kitamura, Y. Wada, S. Yanagida, *J. Photochem. Photobiol., A,* 164 (2004) 153.
11. S. Ahmad, J.H. Yum, Z. Xianxi, M. Gratzel, H.J. Butt, M.K. Nazeeruddin, *J. Mater. Chem.,* 20 (2010) 1654.
12. Q. Li, J. Wu, Q. Tang, Z. Lan, P. Li, J. Lin, L. Fan, *Electrochem. Commun.* 10 (2008) 1299.
13. J. Wu, Q. Li, L. Fan, Z. Lan, P. Li, J. Lin, S. Hao, *J. Power sources* 181 (2008) 172.
14. Y.M. Sun, J.H. Seo, C.J. Takacs, J. Seifter, A.J. Heeger, *Adv. Mater.*, 23 (2011) 1679.
15. R. Sui, P. Charpentier, *Chem. Rev.*, 112 (2012) 3057.
16. L.L Hench, J.K. West, *Chem. Rev.*, 90 (1990) 33.
17. B.O. Regan, M. Gratzel, *Nature*, 353 (1991) 737-740.
18. N. Espinosa, M. Hosel, D. Angmo, F.C. Krebs, *Energy Environ. Sci.,* 5 (2012) 5117.
19. E. Ramasamy, J. Lee, *Carbon* 48 (2010) 3715-3720.

20. M. Schrondner, S. Sensfuss, H. Schache, K. Schultheis, T. Welzel, K. Heinemann, R. Milker, J. Marten, L. Blankenburg, *Sol. Energy Mater. Sol. Cells*, 107 (2012) 283.
21. M. Gao, Y. Xu, Y. Bai, S. Jin, *Appl. Surf. Sci.*, 289 (2014) 145.
22. M. Theuring, M. Vehse, K.V. Maydell, C. Agert, *Thin solid films*, 558 (2014) 294.
23. P. Zhai, Y.H. Chang, Y.T. Huang, T.C. Wei, H. Su, S.P. Feng, *Electrochem. Acta* 132 (2014) 186.
24. S. Woo, S.J. Lee, D.H. Kim, H. Kim, Y. Kim, *Electrochem. Acta* 116 (2014) 518.
25. Y. Zhang, S. Li, D. Zheng, J. Yu, *Organic electronics* 15 (2014) 2647.
26. F. Jay, D. Munoz, T. Desrues, E. Pihan, V.A.D. Oliveira, N. Enjalbert, A. Jouini, *Sol. Energy Mater. Sol. Cells*, 130 (2014) 690.
27. T. Mishima, M. Taguhi, H. Sakata, E. Maruyama, *Sol. Energy Mater. Sol. Cells*, 95 (2011) 18-21.
28. S. Iijima, *Nature*, 354 (1991) 56.
29. H. Choi, H. Kim, S. Hwang, W. Choi, M. Jeon, *Sol. Energy Mater. Sol. Cells* 95 (2011) 323.
30. H. Zhu, J. Wei, K. Wang, D. Wu, *Sol. Energy Mater. Sol. Cells*, 93 (2009) 1461.
31. J.G. Park, M.S. Akhtar, Z.Y. Li, D.S. Cho, W. Lee, O.B. Yang, *Electrochim. Acta*, 85 (2012) 600.
32. Z. Huang, X. Liu, K. Li, Y. Luo, H. Li, W. Song, L.Q. Chen, Q. Meng, *Electrochem. Commun.*, 9 (2000) 596.
33. G.H. Lim, J.M. Zhuo, L.Y. Wong, S.J. Wong, S.J. Chua, L.L. Chua, P.K.H. Ho, *Organic electronics* 15 (2014) 449.
34. D.K. Susarova, A.E. Goryachev, D.V. Novikov, N.N. Dremova, S.M. Peregudova, V.F. Razumov, P.A. Troshin, *Sol. Energy Mater. Sol. Cells*, 120 (2014) 30.
35. R. Sui, P. Charpentier, *Chem. Rev.*, 112 (2012) 3057.
36. T. Kuwabaru, H. Sugiyama, T. Yamaguchi, K. Takahashi, *Thin solid films*, 517 (2009) 3766.
37. M.S. White, D.C. Olson, S.E. Shaleen, N. Kopidakis, D.S. Ginley, *Appl. Phys. Lett.*, 89 (2006) 143517.
38. C. Dunkel, M. Wark, T. Oekermann, R. Ostermann, B.M. Smarsly, *Electrochim. Acta*, 90 (2013) 375.
39. S.B. Kang, J.W. Lim, S.I. Na, H.K. Kim, *Sol. Energy Mater. Sol. Cells*, 107 (2012) 373.
40. N. Wolf, T. Stubhan, J. Manara, V. Dyakonov, C.J. Brabee, *Thin solid films* 564 (2014) 213.
41. N. Bagheri, A. Aghaei, M.Y. Ghotbi, E. Marzbanrad, N. Vlachopolas, L. Haggman, M. Wang, G. Boschloo, A. Hagfelt, M.S. Nuckowska, P.J. Kulesza, *Electrochim. Acta*, 143 (2014) 390.
42. A. Facchetti, *Chem. Mater.*, 23 (2011) 733.
43. P.M. Beaujuge, J.M.J. Frechet, *J. Am. Chem. soc.*, 133 (2011) 20009.
44. A. Colsmann, M. Reinhard, T.H. Kwon, C. Kayser, F. Nickel, J. Czolk, U. Lemmer, N. Clark, J. Jaisieniak, A.B. Holmes, D. Jones, *Sol. Energy Mater. Sol. Cells*, 98 (2012) 118.
45. R. Roesch, K.R. Eberhardt, S. Engmann, G. Gobsch, H. Hoppe, *Sol. Energy Mater. Sol. Cells*, 117 (2013) 59.
46. W. Zhang, C. Min, Q. Zheng, X. Li, J. Fang, *Organic electronics* 15 (2014) 3632.
47. U.J. Lee, S.H. Lee, J.J. Yoon, S.J. Oh, S.H. Lee, J.K. Lee, *Sol. Energy Mater. Sol. Cells*, 108 (2013) 50.
48. R. Ramachandran, V. Mani, S.M. Chen, G. Gnana kumar, M. Govindasamy, *Int. J Electrochem. Sci.*, 10 (2015) 859.
49. K.J. Babu, A. Zahoor, K.S. Nahm, R. Ramachandran, M.A.J. Rajan, G. Gnana kumar, *J. Nanopart. Res.*, 16 (2014) 2250.
50. R. Ramachandran, V. Mani, S.M. Chen, R. Saraswathi, B.S. Lou, *Int. J Electrochem. Sci.*, 8 (2014) 11680.
51. S.M. Chen, R. Ramachandran, V. Mani, R. Saraswathi, *Int. J Electrochem. Sci.*, 9 (2014) 4072.
52. W.Y. Wang, P.N. Ting, S.H. Luo, J.Y. Lin, *Electrochim. Acta*, 137 (2014) 721.
53. P. Zhai, Y.H. Chang, Y.T. Huang, T.C. Wei, H. Su, S.P. Feng, *Electrochim. Acta*, 132 (2014) 186.
54. Y. Zhang, S. Yuan, W. Liu, *Electrochim. Acta*, 143 (2014) 18.

55. T. Stubhan, J. Kuantz, N. Li, F. Guo, I. Litzov, M. Steidl, M. Richter, G.J. Matt, C.J. Brabee, *Sol. Energy Mater. Sol. Cells,* 107 (2012) 248.
56. Y. Zhang, R. Wu, W. Shi, Z. Guen, *Sol. Energy Mater. Sol. Cells,* 111 (2013) 200.
57. K. Xiong, L. Hou, M. Wu, Y. Huo, W. Mo, Y. Yuan, S. Sun, W. Xu, E. Wang, *Sol. Energy Mater. Sol. Cells,* 132 (2015) 252.
58. B.H. Moon, Y.M. Sung, C.H. Han, *Energy procedia* 34 (2013) 589.
59. N.M. Muhammad, S. Sundharam, H.W. Dang, A. Lee, B.H. Ruy, K.H. Choi, *Current applied phys.,* 11 (2011) S68.
60. S. Peng, Y. Wu, P. Zhu, V. Thavalsi, S.G. Mhaisalkar, S. Ramakrishna, *J. Photochem. Photobiol., A,* 223 (2011) 97.
61. M.G. Kang, H.J. Park, S.H. Ahn, L.J. Guo, *Sol. Energy Mater. Sol. Cells,* 94 (2010) 1179.
62. P. Kopola, T. Aernouts, S. Guillerez, H. Jin, M. Tuomikoski, M. Maaninen, J. Hast, *Sol. Energy Mater. Sol. Cells,* 94 (2010) 1673.
63. M.M. Voigt, R.C.I. Mackenzie, S.P. King, C.P. Yau, P. Atienzar, J. Dane, P.E. Keivanidis, I. Zadrazil, D.D.C. Bradley, J. Nelson, *Sol. Energy Mater. Sol. Cells,* 105 (2012) 77.
64. G. Susanna, L. Salamandra, T.M. Brown, A.D. Carlo, F. Brunetti, A. Raale, *Sol. Energy Mater. Sol. Cells,* 95 (2011) 1775.
65. M.M. Voigt, R.C.I. Mackenzie, S.P. King, C.P. Yau, P. Atienzar, J. Dane, P.E. Keivandis, I. Zadrazil, D.D.C. Bradley, J. Nelson, *Sol. Energy Mater. Sol. Cells,* 105 (2012) 77.
66. P. Kopola, B. Zimmermann, A. Filipovic, H.F. Schleiermacher, J. Greulich, S. Rousu, J. Hast, R. Myllyla, V. Wurfel, *Sol. Energy Mater. Sol. Cells,* 107 (2012) 252.
67. K.M. Lee, C.Y. Chen, S.J. Wu, S.C. Chen, C.G. Wu, *Sol. Energy Mater. Sol. Cells,* 108 (2013) 70.
68. X. Chen, C. Jia, Z. Wan, J. Feng, X. Yao, *Organic electronics,* 15 (2014) 2240.
69. Y. Zheng, S. Li, D. Zheng, J. Yu, *Organic electronics,* 15 (2014) 2647.
70. X. Chen, C. Jia, Z. Wan, J. Feng, X. Yao, *Organic electronics,* 15 (2014) 2240.
71. Y. Wang, X. Zhang, H. Zhang, Q. Huang, F. Yang, X. Meng, C. Wei, Y. Zhao, *Sol. Energy Mater. Sol. Cells,* 121 (2014) 49.
72. I.Y.Y. Bu, *Vacuum* 86 (2011) 106.
73. P. Sing, N.M. Ravindra, *Sol. Energy Mater. Sol. Cells,* 101 (2012) 36.
74. C. Xiao, X. Yu, D. Yang, D. Que, *Sol. Energy Mater. Sol. Cells,* 128 (2014) 427.
75. A. Guechi, M. Chegaar, A. Merabet, *Physics procedia,* 21 (2011) 108.
76. A.F. Garcia, R.D. Franco, L. Martinez, J. Wette, *Energy procedia,* 49 (2014) 1682.
77. M.L. Cantu, M.K. Siddiki, D.M. Rojas, R. Amade, N.I.G. Pech, *Sol. Energy Mater. Sol. Cells,* 94 (2010) 1227.
78. Y.X. Nan, F. Chen, L.G. Yang, X.X. Jiang, L.J. Zuo, J.L. Zhang, Q.X. Yan, M.M. Shi, H.Z. Chen, *Sol. Energy Mater. Sol. Cells,* 95 (2011) 3233.
79. T. Gimpel, S. Kontermann, T. Buck, A.L. Baumann, K.M. Gunther, E. Wefringhaus, V. Mihailetchi, E. Lemp, D. Rudolph, J. Theobald, W. Schade, *Energy procedia,* 55 (2014) 186.
80. A. Schneider, N. Traut, M. Hamburger, *Sol. Energy Mater. Sol. Cells,* 126 (2014) 149.
81. W. Hong, Y. Xu, G. Lu, C. Li, G. Shi, *Eelectrochem. Commun.,* 10 (2008) 1555.
82. Q. Tai, B. Chn, F. Guo, S. Xu, H. Hu, B. Sebo, X.Z. Zhao, *ACS Nano,* 5 (2011) 3795.
83. P. Uppachai, V. Harnchana, S. Pimanpang, V. Amornkitbamrung, A.P. Brown, R.M.D. Brydson, *Electrochim. Acta,* 145 (2014) 27.
84. G. Wu, F. Kong, Y. Zhang, X. Zhang, J. Li, W. Chen, W. Liu, Y. Ding, C. Zhang, B. Zhang, J. Yao, S. Dai, *J. Phys. Chem. C,* 118 (2014) 8756.
85. H. Yang, G.H. Guai, C. Guo, Q. Song, S.P. Jiang, Y. Wang, W. Zhang, C.M. Li, *J. Phy. Chem. C,* 115 (2011) 12209.
86. Z. Yin, S. Wu, X. Zhou, X. Huang, Q. Zhang, F. Boey, H. Zhang, *Small,* 6 (2010) 307.
87. M. Dutta, S. Sarkar, T. Ghosh, D. Basak, *J Phys. Chem. C,* 116 (2012) 20127.

88. M.S. Barba, M. Salvandor, A. Kulkarni, D.S. Ginger, A.M. Kelley, *J Phys. Chem. C,* 115 (2011) 20788.
89. D.D. Arhin, M. Fabiane, A. Bello, N. Manyala, *Ind. Eng. Chem. Res.*, 52 (2013) 14160.
90. Y.E. Romanyuk, C.M. Fella, A.R. Uhl, M. Werner, A.N. Tiwari, T. Schnabel, E. Ahlswede, *Sol. Energy Mater. Sol. Cells,* 119 (2013) 181.
91. W. Ke, G. Fang, J. Wang, P. Qin, H. Tao, H. Lei, Q. Liu, X. Dai, X. Zhao, *ACS Applied materials interfaces,* 6 (2014) 15959.
92. L. Kavan, J.H. Yum, M. Gratzel, *ACS Nano,* 5 (2011) 165.
93. A.S. Hart, K.C.C. Bikram, N.K. Subbaiyan, P.A. Karr, F.D. Souza, *ACS Applied matter interfaces,* 4 (2012) 5813.
94. H. Kim, H. Jeong, T.K. An, C.E. Park, K. Yong, *ACS Applied matter interfaces,* 5 (2013) 268.
95. C.H. Lee, W.H. Chiu, K.M. Lee, W.H. Yen, H.F. Lin, W.F. Hsieh, J.M. Wu, *Electrochim. Acta,* 55 (2010) 8422.
96. H.C. Chen, C.C. Lin, H.V. Han, K.J. Chen, Y.L. Tsai, Y.A. Chang, M.H. Shih, H.C. Kuo, P. Yu, *Sol. Energy Mater. Sol. Cells,* 104 (2012) 92.
97. I.H. Choi, C.H. Choi, *Thin solid films,* 525 (2012) 132.
98. J. Greulich, B. Thaidigsmann, S. Rein, *Sol. Energy Mater. Sol. Cells,* 124 (2014) 24.
99. A. Ramar, T. Soundappan, S.-M. Chen, M. Rajkumar, S. Ramiah, *Int. J. Electrochem. Sci.,* 7 (2012) 11734.
100. T.-H. Tsai, C.-Y. Yang, S.-M. Chen, *Int. J. Electrochem. Sci.,* 7 (2012) 12764.
101. T.-H. Tsai, S.-C. Chiou, S.-M. Chen, K.-C. Lin, *Int. J. Electrochem. Sci.,* 6 (2011) 3938.
102. R. Madhu, V. Veeramani, S.-M. Chen, J. Palanisamy, A.T.E. Vilian, *RSC Adv.,* 4 (2014) 63917.
103. T.-H. Tsai, S.-C. Chiou, S.-M. Chen, *Int. J. Electrochem. Sci.,* 6 (2011) 3333.
104. K.-C. Lin, J.-Y. Huang, S.-M. Chen, *Int. J. Electrochem. Sci.,* 7 (2012) 12786.
105. H.W. Choi, N.D. Theodore, T.L. Alford, *Sol. Energy Mater. Sol. Cells,* 117 (2013) 446.
106. Y.K. Lee, C.H. Jung, J. Park, H. Seo, G.A. Somorjai, J.Y. Park, *Nano Lett.,* 11 (2011) 4251.
107. P.R.F. Barnes, A.Y. Anderson, S.E. Koops, J.R. Durrant, B.C.O. Regan. *J Phys. Chem. C,* 113 (2009) 1126.
108. A. Morandeira, J. Fortage, T. Edvisson, L.L. Pleux, E. Blart, G. Boschloo, A. Hagfeldt, L. Hammarstrom, F. Odobel, *J. Phys. Chem. C,* 112 (2008) 1721.
109. T. Trupke, P. Wurfel, *J. Phys. Chem. C,* 104 (2000) 11484.
110. Y. Xue, J. Liu, H. Chen, R. Wang, D. Li, J. Qu, L. Dai, *Angew. Chem. Int. Ed,* 51 (2012) 12124.
111. D.W. Zhang, X.D. Li, H.B. Li, S. Chen, Z. Sun, X.J. Yin, S.M. Huang, *Carbon,* 49 (2011) 5382.
112. W. Guo, C. Xu, X. Wang, S. Wang, C. Pan, C. Lin, Z.L. Wang, *J. Am. Chem. Soc.,* 134 (2012) 4437.
113. X. Yu, X. Yu, J. Zhang, G. Zhao, J. Ni, H. Cai, Y. Zhao, *Sol. Energy Mater. Sol. Cells,* 128 (2014) 307.
114. C. Battaglia, J. Escarre, K. Soderstrom, M. Charriere, M. Despeisse, F.J. Haug, C. Ballif, *Nature,* photonics 5 (2011) 535.
115. Q.Tai, B. Chen, F. Guo, H. Hu, L. Jiang, *ACS Nano,* 5 (2011) 3795.
116. N. Yang, J. Zhai, D. Wang, Y. Chen, L. Jiang, *ACS Nano,* 4 (2010) 887.
117. G.R. Li, F. Wang, Q.W. Jiang, X.P. Gao, P.W. Shen, *Angew. Chem. Int. Ed,* 49 (2010) 3653.
118. F. Gao, Y. Wang, D. Shi, J. Zhang, M. Wang, X. Jing, R.H. Baker, P. Wang, S.M. Zakeeruddin, M. Gratzel, *J. Am. Chem. Soc.,* 130 (2008) 10720.